

# Effect of a Pedicle Screw Fixation System on Lumbar Spinal Segments: A Finite Element Study

## Pedikül Vidalı Sabitleme Sisteminin Lomber Spinal Segmentler Üzerindeki Etkisi: Sonlu Elemanlar Çalışması

<sup>a</sup> Saliha Zeyneb AKINCI<sup>a</sup>, <sup>b</sup> Derya KARABULUT<sup>b</sup>, <sup>c</sup> Suzan Cansel DOĞRU<sup>b</sup>, <sup>d</sup> Hasan Kemal SÜRME<sup>c</sup>,  
<sup>e</sup> Onur YAMAN<sup>d</sup>, <sup>e</sup> Yunus Ziya ARSLAN<sup>e</sup>

<sup>a</sup>Department of Biomedical Engineering and Bioinformatics, İstanbul Medipol University Faculty of Engineering and Natural Sciences, İstanbul, Türkiye

<sup>b</sup>Department of Mechanical Engineering, İstanbul University-Cerrahpaşa Faculty of Engineering, İstanbul, Türkiye

<sup>c</sup>Department of Automotive Technology, İstanbul University-Cerrahpaşa Vocational School of Technical Sciences, İstanbul, Türkiye

<sup>d</sup>Clinic of Brain and Nerve Surgery, Memorial Bahçelievler Hospital, İstanbul, Türkiye

<sup>e</sup>Department of Robotics and Intelligent Systems, Turkish-German University Institute of Graduate Studies in Science and Engineering, İstanbul, Türkiye

**ABSTRACT Objective:** Spinal implants have been used to stimulate fusion by surgical adjustment and correct abnormal alignment of the vertebral column. Spinal fusion can cause some spinal disorders and hence describing the changes in biomechanical forces would help to understand these complications. In this study, we used two lumbar models. One of them is used without the fixed pedicle screw system, and the other one was used with that system. Therefore, we aimed to investigate the biomechanical effect of a pedicle screw fixation system on the lumbar functional spinal unit under applied forces. **Material and Methods:** Computed tomography data of a scoliotic patient was used for the construction of the lumbar models. The second and third vertebrae (L2-L3) of the lumbar spine, two facet joints, an intervertebral disc, and ligaments were constructed. A screw fixation system was employed and Von-Mises stress analysis was carried out for both models. **Results:** The von Mises stress distribution results showed that the presence of fixed implantation transmitted the compressive forces to the screws and rods in all directions and decreased the stress levels considerably by allowing to stabilize the model. The upper side of the L2 vertebra was the most affected region in flexion and lateral bending. However, the pedicle region had the maximum affected area under applied loads in extension and axial rotation. **Conclusion:** It was concluded that a fixed implant system preserves the maintenance of the vertebral column and decreases the stress on the adjacent spinal segments, especially for the intervertebral discs.

**ÖZET Amaç:** Omurga implantları, cerrahi müdahale ile füzyonu hızlandırmaları ve omurganın anormal eğriliğini düzeltmek için kullanılmaktadır. Spinal füzyon bazı spinal bozukluklara neden olabilir ve bu nedenle füzyon ile lomber omurların komşu bölümlerine uygulanan biyomekanik kuvvetlerdeki değişiklikleri açıklamak, bu komplikasyonları anlamaya yardımcı olacaktır. Bu çalışmada iki tane lomber model kullanıldı. Bir tanesi sabit pedikül vida sistemi olmadan kullanıldı, diğeri ise bu sistem ile birlikte kullanıldı. Bu sebeple, bu çalışmada lomber fonksiyonel omurga biriminde pedikül vida sisteminin uygulanan kuvvetler altındaki biyomekanik etkisini araştırmayı amaçladık. **Gereç ve Yöntemler:** Skolyoz bir hastanın bilgisayarlı tomografi verileri lomber omurganın temel birimini oluşturmak için kullanılmıştır. Lomber omurganın ikinci ve üçüncü omurları (L2-L3), iki tane faset eklem, bir tane omurlar arası disk ve bağ dokuları oluşturulmuştur. Bir titanyum vida sabitleme sistemi tasarlanmış ve Von Mises gerilme analizleri in-takt (implant olmayan sistemler) ve implant olan sistemler için uygulanmıştır. **Bulgular:** Von Mises gerilme dağılımı sonuçları, sabit implantasyonun olması durumunda baskı yapan kuvvetlerin vidalara ve çubuklara tüm yönlerde iletiliğini göstermiştir ve gerilme seviyelerini önemli ölçüde azaltarak modelin dengede durmasına olanak sağlamıştır. L2 omurunun en üst bölümünün fleksiyon ve yana eğilmede en fazla etkilenen bölge olmuştur. Ancak uygulanan yükler altındaki ekstansiyon ve aksiyal rotasyonda pedikül bölümü en çok etkilenen alan olmuştur. **Sonuç:** Sabit bir implant sisteminin omurganın bütünlüğünü koruduğu ve özellikle omurlar arası diskler için komşu bölümler üzerindeki gerilmeyi azalttığı sonucuna varılmıştır.

**Keywords:** Spine; lumbar vertebrae; finite element analysis; pedicle screws

**Anahtar Kelimeler:** Omurga; lomber omur; sonlu eleman analizi; pedikül vidaları

**Correspondence:** Saliha Zeyneb AKINCI

Department of Biomedical Engineering and Bioinformatics, İstanbul Medipol University Faculty of Engineering and Natural Sciences, İstanbul, Türkiye

**E-mail:** szakinci@medipol.edu.tr



Peer review under responsibility of Türkiye Klinikleri Journal of Medical Sciences.

**Received:** 09 Aug 2023

**Received in revised form:** 22 Oct 2023

**Accepted:** 29 Nov 2023

**Available online:** 01 Dec 2023

2146-9040 / Copyright © 2023 by Türkiye Klinikleri. This is an open access article under the CC BY-NC-ND license (<http://creativecommons.org/licenses/by-nc-nd/4.0/>).

Scoliosis is defined as the three-dimensional deformity of the vertebral column.<sup>1</sup> Abnormal curvature of the spine leads to the degeneration of the intervertebral discs and facet joints in the long term of this deformation, and the misalignment of the spine usually causes pain, especially in the lumbar and lower thoracic regions of the patients.<sup>2</sup>

It has been observed that the deformation of the spine has decreased when compressive forces have been applied across the intervertebral disc spaces, and this has led researchers to investigate the effect of different corrective forces in the stabilization of the spine.<sup>3</sup> Surgical procedure (especially, spinal fusion) that requires correction with the attachment of rods to the spine by using screws inserted into the vertebral bodies is the most preferred strategy to decrease the pain and correct the misalignment.<sup>4</sup>

To provide stability and homogeneous load sharing between anterior and posterior ligaments, a rigid fixation system has been used in spine surgeries.<sup>5-7</sup> While spinal fusion eliminates the relative motion between two vertebrae and may prevent back pain, complications of spinal fusion may develop after spinal fusion.<sup>8-11</sup> When one or more vertebrae are fused and no longer move in the vertebral column, the spinal units above and below the spinal fusion compensate for lost motion at the fused level, which increases adjacent segments' mobility, and hence leads to wear and tear over the adjacent segment. Biomechanical analysis of a spine that was subjected to spinal fusion may provide an opportunity to better evaluate the effect of such spinal disorders.

Accordingly, some finite element-based biomechanical studies have attempted to gain insight into the effect of spinal fusion on the spine.<sup>4-7,11-14</sup> For example, several researchers studied the posterior lumbar interbody fusion to investigate the stress on the nerve roots in the spine.<sup>12</sup> Additionally, the biomechanical compatibility of interlaminar and interspinous devices was compared in another study to analyze the effect of the position of these instruments in the treatment of surgical decompression.<sup>13</sup>

The spinal motion segment, which is also known as the functional spinal unit, describes the whole characteristic behavior of the spinal column.<sup>15</sup> In

order to understand the condition of the entire vertebral column, especially in a scoliotic spine, this smallest segment needs to be studied to describe the effect of fixed instrumentation on the spine. Therefore, the objective of this study was to investigate the biomechanical effect of a pedicle screw fixation system on the L2-L3 lumbar spine model. A finite element lumbar model was developed and a rigid rod and pedicle screw fixation system were integrated into the lumbar model to simulate the fusion process of the lumbar spinal unit region.

## MATERIAL AND METHODS

The construction process of the model that was employed in this study was completed for each spinal element of the model. The spinal unit of this study is composed of two lumbar vertebrae with cortical and trabecular regions, seven spinal ligaments [anterior longitudinal ligament (ALL), posterior longitudinal ligament (PLL), interspinous ligament (ISL), supraspinous ligament (SSL), ligamentum flavum (LF), intertransverse ligament (ITL)], facet joints, and also intervertebral discs with annulus and nucleus parts.<sup>16</sup>

In spinal kinematics and computational spinal research, the basic spinal unit to be studied involves 2 vertebrae and an intervertebral disc between them.<sup>17</sup> Therefore, in the current the development of the lumbar spinal unit of the L2-L3 model was completed and von Mises stresses were calculated over the spinal unit and the implant system.

This study complies with the Declaration of Helsinki and was performed according to ethics committee approval. Ethical approval for this study was taken from the Non-Invasive Clinical Research Ethics Committee (decision number: 414) on 15 August 2018 at İstanbul Medipol University, İstanbul, Türkiye.

## CONSTRUCTION OF THE THREE-DIMENSIONAL MODEL

Computed tomography (CT) data from a patient with scoliosis using a CT scanner (Siemens/Somat Definition AS) with a slice thickness of 1.50 mm was employed for the construction of the spinal unit model. The functional spine unit model was obtained from these two-dimensional stacked images and then

converted into three-dimensional (3D) objects by using medical image processing software (Mimics, Materialise's Interactive Medical Image Control System, Belgium). **Figure 1** shows the reconstruction process in axial, coronal, and sagittal planes.

The two-motion segment (L2-L3 lumbar vertebrae model) with all spinal components was constructed step by step with the help of several computer programs Mimics and 3-matic software (Mimics, Materialise's Interactive Medical Image Control System, Belgium) and Ansys workbench software (ANSYS 16.0, Ansys Inc. Canonsburg, PA, USA). In order to reconstruct the bone structure of the lumbar spine, preset thresholds were used. The range of the threshold was between 226-3071 Hounsfield Unit for the construction of lumbar vertebral bones. Manual editing tools such as cropping the mask, morphology operations, and multi-slice editing were also employed for the rest of the spinal structures, except the ligaments. In the end, different segmentation masks were used for the construction of the two lumbar vertebrae, two facet

joints, and an intervertebral disc. All of the spinal components were obtained and saved as stp files.

In the construction of the vertebral bodies, as a first step, the full structure of the bodies was obtained and then smoothed without changing the details of the structures (**Figure 1**). Then stl files of the bony structures were imported into the 3-matic software (Mimics, Materialise's Interactive Medical Image Control System, Belgium). An offset value of 1 mm was applied to all vertebral models to separate the trabecular and the cortical bone regions (**Figure 2**).<sup>12</sup> The stp files were then imported into Ansys workbench software and in the Design Modeler section of this software, the trabecular and cortical regions were selected and recorded as a new part. By doing so, the vertebral bodies involved both trabecular and cortical sections before the finite element analysis.

In addition to this process, the intervertebral disc was also constructed. The disc was modeled to consist of two different parts, namely the annulus fibrosus and the nucleus pulposus (**Figure 3**). The nucleus pulposus was constructed as a cylinder in the disc structure, and the surrounding volume around the nucleus was constructed as the annulus region of the intervertebral disc.<sup>18-20</sup> Like the vertebral bodies, these two structures of the disc were saved as one part in the "Model" section of the software (**Figure 3**).

#### CONSTRUCTION OF THE LIGAMENTS

The ligaments (anterior and posterior longitudinal, interspinous, supraspinous, LF, and ITLs) of the L2-L3 lumbar model were constructed as linear single-force components. In the standing posture of the body, the slack length of these structures was defined, and while stretching the body these components generate a tensile force beyond this length.<sup>21,22</sup> All the corresponding ligaments of the lumbar model were defined as spring units.<sup>21,22</sup> The stiffness parameters of the ITLs were not included in this study. These values were taken from literature which are based on in-vitro studies on human cadavers (**Table 1**).<sup>22,23</sup>

#### CONSTRUCTION OF THE PEDICLE SCREWS AND RODS

For the generation of the pedicle screws, cylindrical shapes were used with the help of the "analyze" sec-

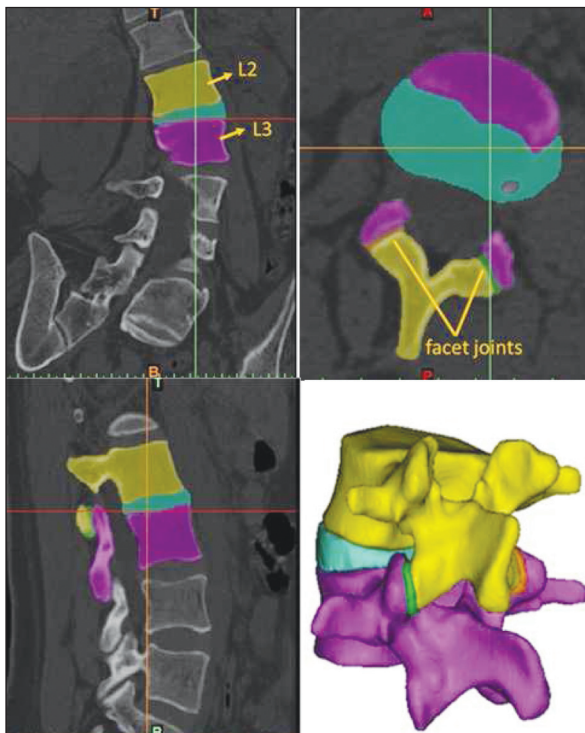


**FIGURE 1:** The segmentation process of the lumbar vertebrae (L2 and L3) and also the intervertebral disc that separates them in coronal (a), axial (b), and sagittal planes (c). The 3D model was obtained after the segmentation (d). 3D: Three-dimensional.

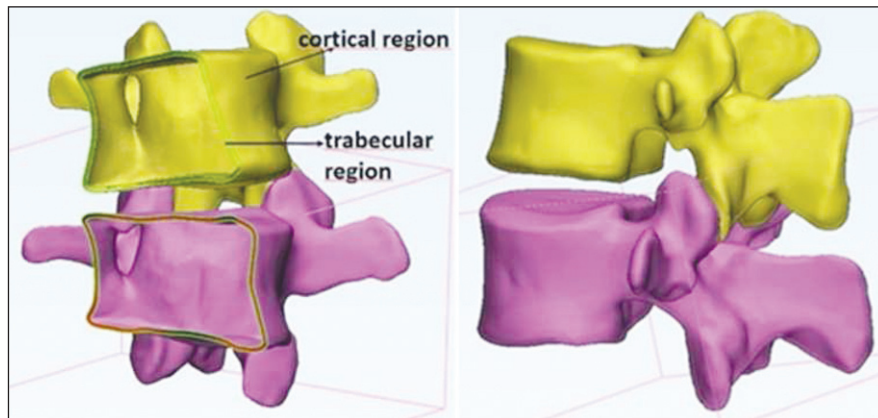


**FIGURE 2:** The representation of the (a) trabecular (the inner shell) and cortical (the outer shell) regions of the lumbar vertebrae (L2 and L3), and (b) the 3D full structure of the model. 3D: Three-dimensional.

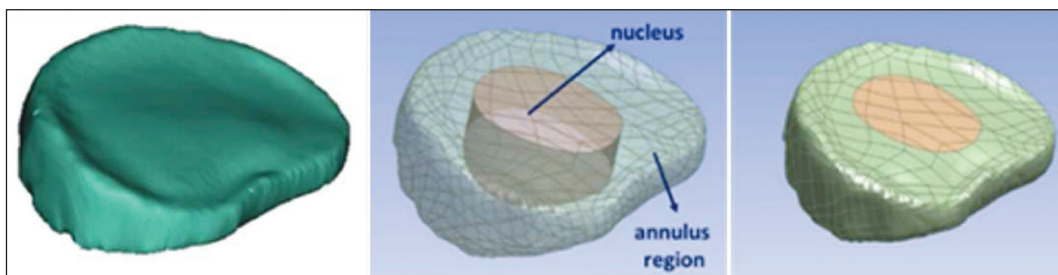


**FIGURE 3:** The representation of the L2-L3 full intervertebral disc obtained from segmentation (a). The annulus and nucleus regions were separated in Ansys software (b and c).

**TABLE 1:** Stiffness values of the ligaments that were experimentally obtained.<sup>22,23</sup>

Ligament	Stiffness (N/mm)
ALL	20.8±14.0
PLL	36.6±15.2
ISL	9.6±4.8
SSL	24.8±14.5
LF	25.1±10.9
IT	50.0

The abbreviations for the structures are as follows; ALL: Anterior longitudinal ligament; PLL: Posterior longitudinal ligament; ISL: Interspinous ligament; SSL: Supra-spinous ligament; LF: Ligamentum flavum; IT: Intertransverse ligament.

tion in Mimics software. The interaction of the screws and bones was assigned to be constrained. The pedicle screw trajectories were adjusted on the second (L2) and third (L3) lumbar vertebrae (Figure 4).

The length (60 mm), the operation angles, and also the radius (2.5 mm) of the screws were all manually adjusted in the software. Also, two rods were designed with the same procedure as the pedicle

screws. The rods had a length of 55 mm and a radius of 1.8 mm. Titanium was assigned as the material for rods and screws in the study.

## MATERIAL PROPERTIES OF THE COMPONENTS

The modulus of elasticity and Poisson's ratio for each spinal unit component (including pedicle screws and rods) were defined in the material library section of Ansys software. Before the simulation process, the materials were assigned to each part of the model in the mechanical section of the software (Table 2).<sup>12,13,16,24</sup>

## MESHING

The meshing of the L2-L3 lumbar model (with/without the implant) was performed using the Ansys software (Ansys Workbench 16.0). The L2-L3 model without any implant system involved 494,907 nodes and 331,453 elements. The number of elements of the model with the fixed implant system was 154,679 elements and it had 238,562 nodes. In the meshing pro-

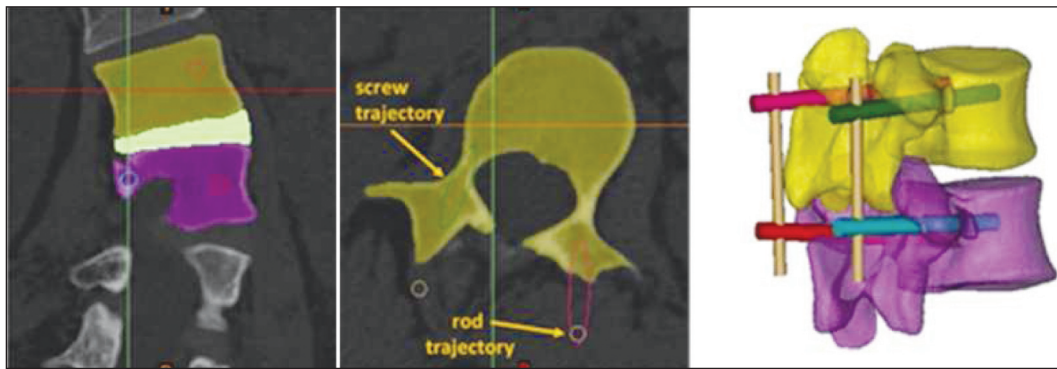


FIGURE 4: The representation of the screw and rod trajectories in (a) coronal, and (b) axial regions of the fixed implant system, (c) that was inserted into the L2-L3 model.

TABLE 2: Material properties of the tissues and implants.

Modeled tissues and spinal devices	Young's modulus (MPa)	Poisson's ratio	Element type	Reference
Cancellous bone	100	0.2	10-node tetrahedral element	13,24
Cortical bone	12,000	0.3	10-node tetrahedral element	13,16,24
Nucleus pulposus	1	0.499	10-node tetrahedral element	13,16,24
Annulus ground	8	0.49	10-node tetrahedral element	12
Implants (screws and rods)	110,000	0.3	10-node tetrahedral element	13,24

cess of all of these models, a 10-node tetrahedral mesh was used (Table 2).

#### BOUNDARY AND LOADING CONDITIONS

A combination of a moment (8 Nm) and a compression force (500 N) was applied to the lumbar models with and without a fixed implant system as the loading condition. To mimic the directional movements, the pure moment including flexion, extension, lateral bending, and axial rotation moments were applied to the model separately. Applied compression force was related to the local muscle forces and the body weight. In order to load the two-segment model, the lowest part of the L3 vertebra was fixed, and the loads were applied to the top section of the L2 vertebra.

#### VALIDATION OF THE FINITE ELEMENT MODEL

Validation of a finite element model by taking the experimental data into account would improve the accuracy of the interpretation of the simulation results. Accordingly, we validated the simulation results by comparing them with the experimental results in the literature under identical loading and boundary conditions.<sup>25</sup> For the validation of the intact (without im-

plant systems) and implanted L2-L3 finite element models, the range of motion (ROM) in flexion, extension, lateral bending, and axial rotation were compared with the published experimental data.<sup>25</sup>

## RESULTS

#### VALIDATION RESULTS

ROM obtained from the lumbar model used in this study and experimental study from the literature with and without the fixed implant system in all directions were given (Figure 5).<sup>25</sup> The ROM values for the L2-L3 model without the implant system was 2.7° for flexion, 2.4° for extension, 3.0° for lateral bending, and 2.6° for axial rotation in this study (Figure 5). For extension motion, the resulting ROM values of our model were in the range of the experimental results from the literature.<sup>25</sup> Similarly, for lateral bending motion, ROM values were consistent with the in vivo experimental results.<sup>25</sup>

The validation of the L2-L3 model with the fixed implant system under flexion, extension, lateral bending, and axial rotation was also investigated. The ROM values for the implanted model were 2.3° for

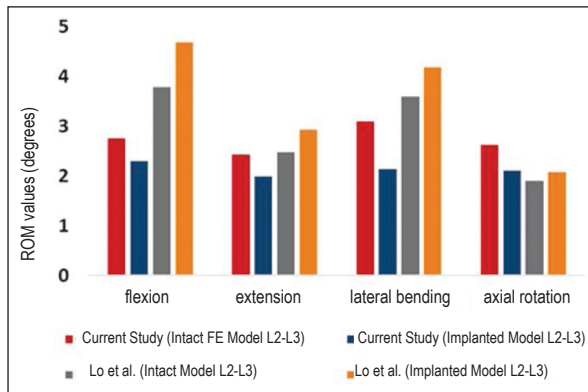


**FIGURE 5:** The comparison of the ROM values of the assembly structure of the L2-L3 normal lumbar model with all the spinal components, and the models with the pedicle screw fixation system. ROM: Range of motion.

flexion, 2.0° for extension, 2.1° for lateral bending, and 2.1° for axial rotation (Figure 5). For axial rotation and extension motions, ROM results were consistent with the literature, especially for axial motion, the results were consistent with the experiment.<sup>25</sup> The computational ROM values in the implanted system were less than those of experimentally obtained ones for flexion and lateral bending, but generally, they were in the range of the developed model.

### von MISES STRESS DISTRIBUTION RESULTS

For all 4 movement directions, the equivalent von Mises stresses over the intervertebral discs were calculated for the models with and without spinal implantation. In the finite element analysis, color changes in the models represent the intensity of the mechanical stress in flexion, extension, lateral bending, and axial rotation.

According to the results, the L2-L3 intervertebral disc displayed the maximum stress in flexion with  $1.67 \times 10^6$  MPa (Figure 6). This result is similar to the peak stress value in extension movement. However, in lateral bending and axial rotation, von Mises stress values of the intervertebral disc decreased to  $1.47 \times 10^6$  MPa and  $1.28 \times 10^6$  MPa, respectively (Figure 6).

The stress distribution over the intervertebral disc in the model with the spinal implantation resulted in lower von Mises stress values compared to the intact model. The maximum stress in flexion was recorded as 1.32 MPa (Figure 7). Similar stress results were found in extension and axial rotation as 0.86 MPa and 0.88 MPa, respectively (Figure 7). Also, the von Mises stress result was 1.04 MPa for lateral bending with the spinal implantation system (Figure 7).

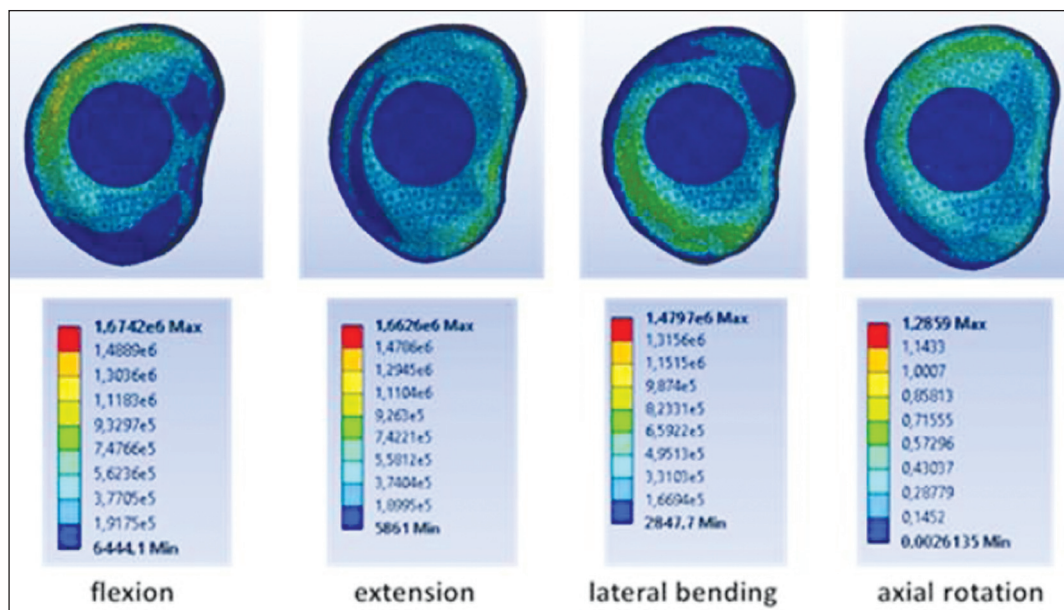


**FIGURE 6:** The representation of von Mises stress analysis of the intervertebral disc of the L2-L3 model (without implant) under loading conditions. The physiological movements of the model as flexion, extension, lateral bending, and axial rotation were given.

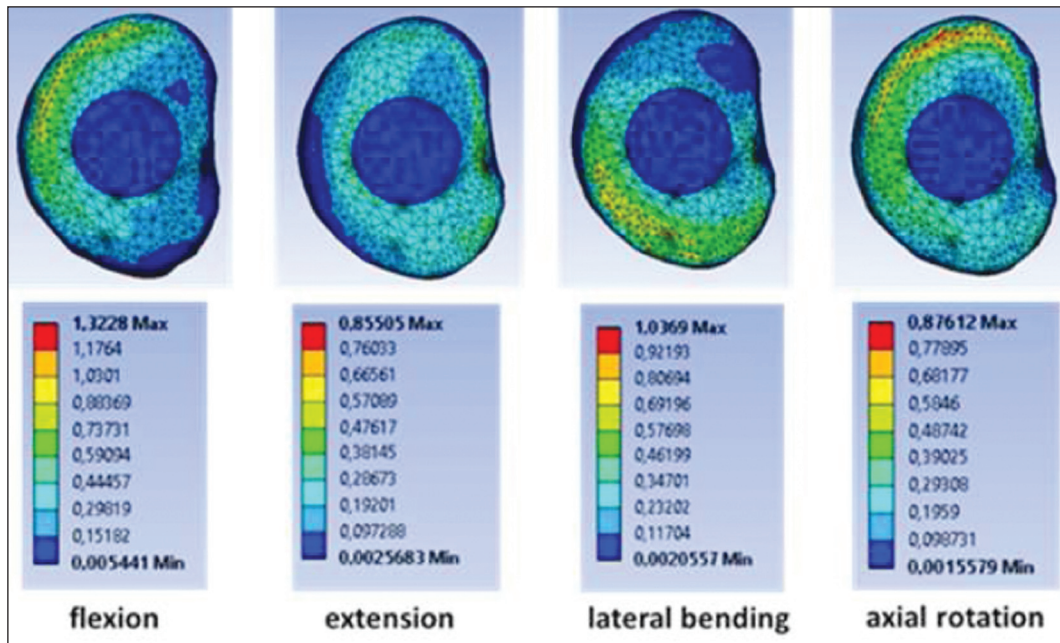


**FIGURE 7:** The representation of von Mises stress analysis of the intervertebral disc of the L2-L3 model (with fixed implant) under loading conditions. The physiological movements of the model as flexion, extension, lateral bending, and axial rotation were given.

The affected regions of the L2-L3 lumbar model without the fixed implant system were investigated (Figure 8). According to the color-coded map of von Mises stress results, intensity changes were seen generally in extension, lateral bending, and axial rotation. Mechanical stress was recorded as much higher in lateral bending. The upper vertebra (L2) also indicated stress on its top surface, especially in lateral bending and flexion. The pedicle regions showed high-stress areas in extension, lateral bending, and axial rotation with higher intensity regions than the other sections of the model (Figure 8).

The affected regions of the L2-L3 lumbar model with the pedicle screw implant system under loading and boundary conditions and the stress values were also studied (Figure 9a). Stress distribution according to the color-changing areas was also recorded on the screws and rods during flexion, extension, lateral bending, and axial rotation (Figure 9b). Unlike the model without the spinal implantation, no significant stress values were noted on the pedicle screws for all movement directions with the fixed spinal implantation. Besides, the color-coded map indicated that intensity changes were seen higher in axial rotation and flexion, and these intensity

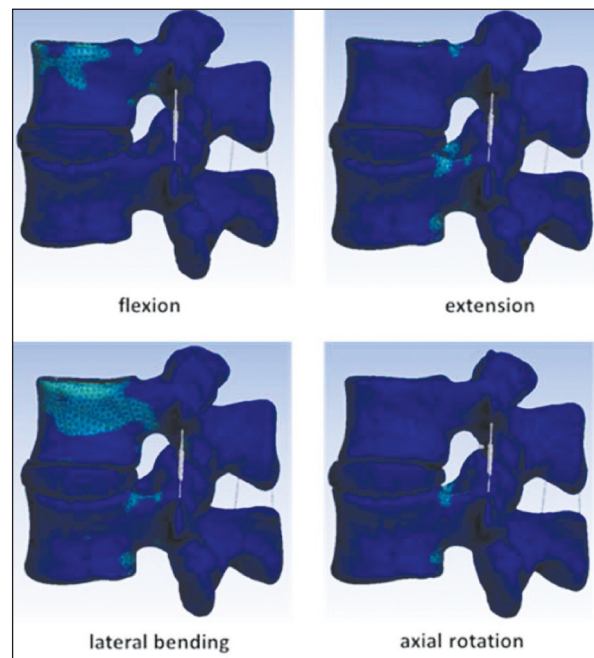


**FIGURE 8:** The affected regions of the L2-L3 lumbar model (without the implant system) under loading and boundary conditions for flexion, extension, lateral bending, and axial rotation.

changes were found in all screws and rods of the system. Additionally, lower stress distribution was observed during extension and lateral bending (Figure 9).

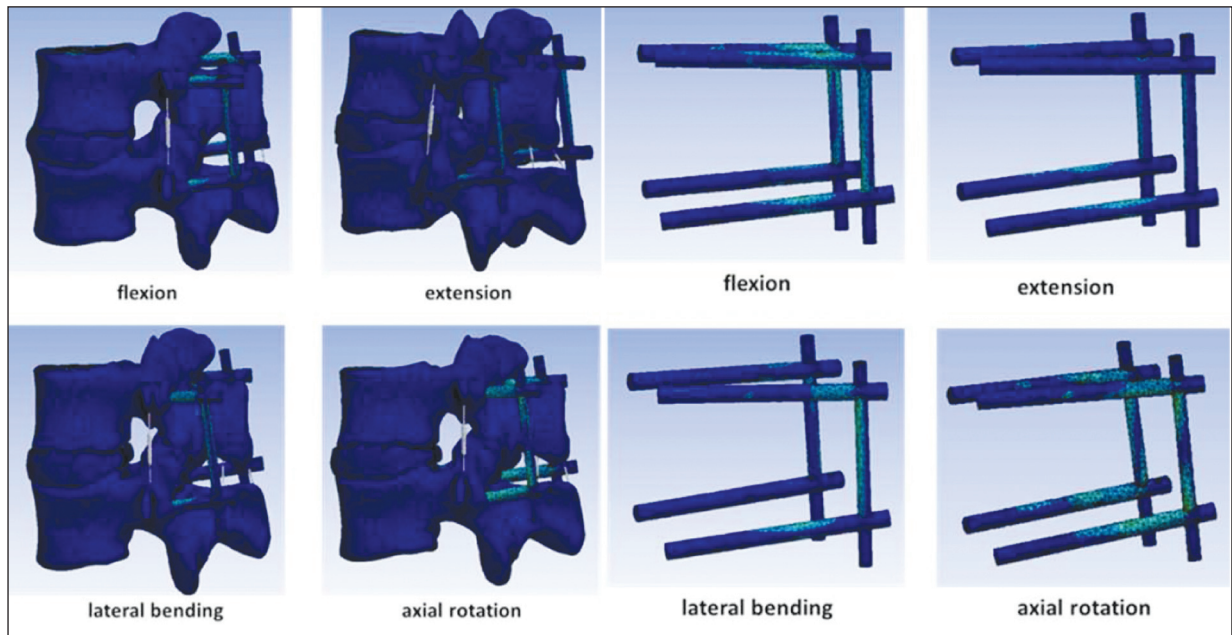


**FIGURE 9:** The affected regions of the (a) L2-L3 lumbar model (with the pedicle screw implant system) under loading and boundary conditions and the stress values distributed on the (b) screws and rods during flexion, extension, lateral bending, and axial rotation.

## DISCUSSION

In this study, a detailed 3D finite element lumbar model was developed for a patient suffering from adolescent idiopathic scoliosis. We studied the biomechanical behavior of a fixed traditional titanium screw-rod system and analyze the influence of the implant system over the whole spinal elements in the model including vertebrae, intervertebral disc, screw, and rod models in terms of von Mises stress distribution. Compression load and pure moments were applied in 4 directions including flexion, extension, lateral bending, and axial rotation.

The L2-L3 lumbar model of the current study was validated by comparing the simulation results with the experimental data in the literature (Figure 5). The ROM results reported in the current study were generally consistent with the experimental data taken from the literature, especially in extension and axial rotation.<sup>24</sup> Also, slightly different values of ROM were found in flexion and lateral bending but these values were similar to the previous studies reported in this study (Figure 5).

Additionally, the von Mises stress distribution results on the intervertebral without the implantation

system were compared for the two models. The comparison of the finite element analysis results of the two models indicated that in all four movement directions including flexion, extension, lateral bending, and axial rotation, there were higher stress results on the L2-L3 intervertebral disc without the pedicle-screw implantation system (Figure 6). However, von Mises stress analysis results on the other model with the implant system recorded lower stress values on the intervertebral disc (Figure 7).

The stress on the whole functional spinal unit (the L2-L3 model) indicates that the upper side of the L2 vertebra was the most affected region in flexion and lateral bending (Figure 8). However, the pedicle region had the maximum affected areas under compressive loads and moments in extension and axial rotation (Figure 8).

In the current study, the axial compression force and moment were applied to the finite element models with and without the fixed pedicle-screw implantation system. And these applied forces were transferred through the L2-L3 lumbar spine model with titanium rods and screws. According to the results, the existence of the screw-rod fixation system on the model reduced the equivalent von Mises stress

values. The maximum stress was transferred to the rods in each movement of the model, but the highest values of stress were recorded in flexion, lateral bending, and axial rotation (Figure 9). The results showed that the fixed implant had the maximum stress on rods, especially in flexion, extension, and axial rotation. The smallest von Mises equivalent stress of the implant appeared in extension. The stress distribution of the titanium implants in various motions indicated that the ROM is less in the implanted model when compared with the intact model (Figure 9). This result showed that the fixed implant system led to a stiff lumbar model and thus, the stress values were below those of the model without the implant system. According to the finite element analysis with the fixed implant system, the total deformation and stress values were decreased on the L2-L3 intervertebral disc when compared with the model without the implant system. The maximum stress values were recorded especially on the rods and also on the screw-rod interfaces in all models (with/without implant system). Furthermore, in both of these models, the fixation system allowed the stabilization of the L2-L3 lumbar spine model. Therefore, the whole model with the implant system showed lower von Mises stress results on the L2-L3 intervertebral disc, and it was observed that the rods and the screws were the most affected parts of the model. When the comparison was done, the model without the implant system displayed higher stress distribution, especially in the intervertebral disc and the pedicle regions of the vertebrae.

This study includes several limitations. One of them was the lack of collagen fibers in the annulus region of the intervertebral disc. Additionally, the material properties of the nucleus pulposus were taken as isotropic and elastic in the simulation. If the disc structure was modeled with these fibers, along with the hyperelastic material properties, the finite element model could have more reflected the actual structure. However, the fact that such modeling preferences are almost unobtainable experimentally limits their use. Another limitation was related to the construction process. Our study has patient-specific

characteristics, thus the CT scan data of one patient was used in all construction and simulation processes. The other limitation was the absence of muscle tissues in the whole lumbar model. If the muscles were included in the model, the finite element analysis could be enhanced in the study. However, since it is technically not appropriate to model muscles from CT scan data, we could not model muscle tissues.

## CONCLUSION

It was concluded that a fixed implant system preserves the maintenance of the vertebral column and decreases the stress on the spinal unit, especially for the intervertebral disc. This study is expected to contribute to future biomechanical studies including the effects of modeling strategies and features of the spinal implantations to the finite element models for further mechanical analysis.

### Source of Finance

*During this study, no financial or spiritual support was received neither from any pharmaceutical company that has a direct connection with the research subject, nor from a company that provides or produces medical instruments and materials which may negatively affect the evaluation process of this study.*

### Conflict of Interest

*No conflicts of interest between the authors and / or family members of the scientific and medical committee members or members of the potential conflicts of interest, counseling, expertise, working conditions, share holding and similar situations in any firm.*

### Authorship Contributions

**Idea/Concept:** Yunus Ziya Arslan, Onur Yaman, Saliha Zeyneb Akinci; **Design:** Yunus Ziya Arslan, Onur Yaman, Saliha Zeyneb Akinci, Hasan Kemal Sürmen; **Control/Supervision:** Yunus Ziya Arslan, Saliha Zeyneb Akinci; **Data Collection and/or Processing:** Onur Yaman, Saliha Zeyneb Akinci; **Analysis and/or Interpretation:** Yunus Ziya Arslan, Onur Yaman, Saliha Zeyneb Akinci, Derya Karabulut, Hasan Kemal Sürmen, Suzan Cansel Doğru; **Literature Review:** Yunus Ziya Arslan, Onur Yaman, Saliha Zeyneb Akinci, Hasan Kemal Sürmen; **Writing the Article:** Saliha Zeyneb Akinci; **Critical Review:** Yunus Ziya Arslan, Saliha Zeyneb Akinci.

## REFERENCES

- Janicki JA, Alman B. Scoliosis: Review of diagnosis and treatment. *Paediatr Child Health*. 2007;12(9):771-6. [[Crossref](#)] [[PubMed](#)] [[PMC](#)]
- Zheng J, Yang Y, Lou S, Zhang D, Liao S. Construction and validation of a three-dimensional finite element model of degenerative scoliosis. *J Orthop Surg Res*. 2015;10:189. [[Crossref](#)] [[PubMed](#)] [[PMC](#)]
- Little JP, Izatt MT, Labrom RD, Askin GN, Adam CJ. An FE investigation simulating intra-operative corrective forces applied to correct scoliosis deformity. *Scoliosis*. 2013;8(1):9. [[Crossref](#)] [[PubMed](#)] [[PMC](#)]
- Gong Z, Chen Z, Feng Z, Cao Y, Jiang C, Jiang X. Finite element analysis of 3 posterior fixation techniques in the lumbar spine. *Orthopedics*. 2014;37(5):e441-8. [[Crossref](#)] [[PubMed](#)]
- Chen CS, Huang CH, Shih SL. Biomechanical evaluation of a new pedicle screw-based posterior dynamic stabilization device (Awesome Rod System)-a finite element analysis. *BMC Musculoskelet Disord*. 2015;16:81. [[Crossref](#)] [[PubMed](#)] [[PMC](#)]
- Panjabi MM, White AA. *Clinical Biomechanics of Spine*. 2nd ed. Baltimore, MD: J.B. Lippincott Company; 1990.
- Herren C, Beckmann A, Meyer S, Pishnamaz M, Mundt M, Sobottke R, et al. Biomechanical testing of a PEEK-based dynamic instrumentation device in a lumbar spine model. *Clin Biomech (Bristol, Avon)*. 2017;44:67-74. [[Crossref](#)] [[PubMed](#)]
- Ishihara H, Kanamori M, Kawaguchi Y, Nakamura H, Kimura T. Adjacent segment disease after anterior cervical interbody fusion. *Spine J*. 2004;4(6):624-8. [[Crossref](#)] [[PubMed](#)]
- Kashkoush A, Agarwal N, Paschel E, Goldschmidt E, Gerszten PC. Evaluation of a hybrid dynamic stabilization and fusion system in the lumbar spine: a 10 year experience. *Cureus*. 2016;8(6):e637. [[Crossref](#)] [[PubMed](#)] [[PMC](#)]
- Saavedra-Pozo FM, Deusdara RA, Benzel EC. Adjacent segment disease perspective and review of the literature. *Ochsner J*. 2014;14(1):78-83. [[PubMed](#)] [[PMC](#)]
- Zhou C, Cha T, Li G. An upper bound computational model for investigation of fusion effects on adjacent segment biomechanics of the lumbar spine. *Comput Methods Biomech Biomed Engin*. 2019;22(14):1126-34. [[Crossref](#)] [[PubMed](#)]
- Fan Y, Zhou S, Xie T, Yu Z, Han X, Zhu L. Topping-off surgery vs posterior lumbar interbody fusion for degenerative lumbar disease: a finite element analysis. *J Orthop Surg Res*. 2019;14(1):476. [[Crossref](#)] [[PubMed](#)] [[PMC](#)]
- Lu T, Lu Y. Interlaminar stabilization offers greater biomechanical advantage compared to interspinous stabilization after lumbar decompression: a finite element analysis. *J Orthop Surg Res*. 2020;15(1):291. [[Crossref](#)] [[PubMed](#)] [[PMC](#)]
- Song M, Sun K, Li Z, Zong J, Tian X, Ma K, et al. Stress distribution of different lumbar posterior pedicle screw insertion techniques: a combination study of finite element analysis and biomechanical test. *Sci Rep*. 2021;11(1):12968. [[Crossref](#)] [[PubMed](#)] [[PMC](#)]
- Iorio JA, Jakoi AM, Singla A. Biomechanics of degenerative spinal disorders. *Asian Spine J*. 2016;10(2):377-84. [[Crossref](#)] [[PubMed](#)] [[PMC](#)]
- Salsabili N, Santiago López J, Prieto Barrio MI. Simplifying the human lumbar spine (L3/L4) material in order to create an elemental structure for the future modeling. *Australas Phys Eng Sci Med*. 2019;42(3):689-700. [[Crossref](#)] [[PubMed](#)]
- Tyndyk MA, Barron V, McHugh PE, O'Mahoney D. Generation of a finite element model of the thoracolumbar spine. *Acta Bioeng Biomech*. 2007;9(1):35-46. [[PubMed](#)]
- Coogan JS, Francis WL, Eliason TD, Bredbenner TL, Stemper BD, Yoganandan N, et al. Finite element study of a lumbar intervertebral disc nucleus replacement device. *Front Bioeng Biotechnol*. 2016;4:93. [[Crossref](#)] [[PubMed](#)] [[PMC](#)]
- Khademi M, Mohammadi Y, Gholampour S, Fatouree N. The nucleus pulposus of intervertebral disc effect on finite element modeling of spine. *International Clinical Neuroscience Journal*. 2016;3(3):150-7. [[Link](#)]
- Maquer G. Meshing of intervertebral discs and cement in smooth models of vertebrae. *Vienna University of Technology*. 2011:1-42. [[Link](#)]
- Chazal J, Tanguy A, Bourges M, Gaurel G, Escande G, Guillot M, et al. Biomechanical properties of spinal ligaments and a histological study of the supraspinal ligament in traction. *J Biomech*. 1985;18(3):167-76. [[Crossref](#)] [[PubMed](#)]
- Putzer M, Auer S, Malpica W, Suess F, Dendorfer S. A numerical study to determine the effect of ligament stiffness on kinematics of the lumbar spine during flexion. *BMC Musculoskelet Disord*. 2016;17:95. [[Crossref](#)] [[PubMed](#)] [[PMC](#)]
- Pintar FA, Yoganandan N, Myers T, Elhagediab A, Sances A Jr. Biomechanical properties of human lumbar spine ligaments. *J Biomech*. 1992;25(11):1351-6. [[Crossref](#)] [[PubMed](#)]
- Liu C, Kamara A, Yan Y. Investigation into the biomechanics of lumbar spine micro-dynamic pedicle screw. *BMC Musculoskelet Disord*. 2018;19(1):231. [[Crossref](#)] [[PubMed](#)] [[PMC](#)]
- Lo CC, Tsai KJ, Chen SH, Zhong ZC, Hung C. Biomechanical effect after Coflex and Coflex rivet implantation for segmental instability at surgical and adjacent segments: a finite element analysis. *Comput Methods Biomech Biomed Engin*. 2011;14(11):969-78. [[Crossref](#)] [[PubMed](#)]